*J. Fluid Mech.* (2005), *vol.* 541, *pp.* 383–397.  
doi:10.1017/S0022112005006300 Printed in the United Kingdom

# Asymptotic analysis of the near-wall region of turbulent natural convection flows

By M. HÖLLING AND H. HERWIG

Hamburg University of Technology, Applied Thermodynamics, Denickestrasse 17, D-21073 Hamburg, Germany

(Received 21 July 2004 and in revised form 27 May 2005)

High-Grashof-number turbulent natural convection in the vicinity of vertical walls with heat transfer is analysed asymptotically. The near-wall boundary layer has a viscosity-influenced inner layer and a fully turbulent outer layer, similar to the structure of forced convection boundary layers. Scaling laws and wall functions are found by asymptotic matching of the temperature gradients in the overlap layer. The temperature wall function then is a simple logarithmic function of wall distance whereas the velocity profile in the overlap layer is a more complex correlation. Constants in these wall functions are deduced from high-quality data for large Grashof numbers. Experimental as well as numerical profiles as a whole are very well reproduced by the combination of wall functions and viscous sublayer profiles. Therefore these new asymptotic profiles can be used in CFD codes to avoid very fine grids close to the wall, when Grashof numbers are high.

## 1. Introduction

Turbulent natural convection along vertical walls is a frequently encountered flow situation for example in air conditioning of buildings, cooling of electronic devices or nuclear power plants. Often Grashof numbers are very large for these flows. Here, the Grashof number is $Gr = g\beta\Delta T h^3/\nu^2$, with $g$ being the gravitational accelaration, $\beta$ the thermal expansion coefficient, $\Delta T$ a characteristic temperature difference, $h$ a geometrical length scale (channel height or distance along the plate) and $\nu$ the kinematic viscosity. Alternatively the Rayleigh number $Ra = Gr\,Pr$ can be used with the molecular Prandtl number $Pr = \nu/a$ and the thermal diffusivity $a$.

For an asymptotic analysis ($Gr \to \infty$ or $Ra \to \infty$) of such flows it is important to have high-quality experimental and/or numerical data to validate the proposed functions and to obtain the model constants involved. There are three standard geometries with heat transfer at vertical walls. One is a vertical channel of infinite extent between a heated and a cooled wall, see figure 1(*a*). This simple geometry has been extensively investigated using direct numerical simulation (DNS) by Versteegh & Nieuwstadt (1999), Boudjemadi *et al.* (1997) and Wang, Fu & Zhang (2002) and experimentally by Betts & Bokhari (2000). The second standard geometry is a hot vertical plate in an environment at rest, studied by e.g. Tsuji & Nagano (1988*a*, *b*), Tsuji, Nagano & Tagawa (1991), and Cheesewright (1968) and for non-Boussinesq conditions by Siebers, Moffatt & Schwind (1985), see figure 1(*b*). The third standard geometry is that of a cavity with sidewalls at different temperatures and a small aspect ratio as studied by Ampofo & Karayiannis (2003) and Cheesewright, King & Ziai (1986). All experimental and numerical data used in our study are for air with a Prandtl number $Pr = 0.71$.

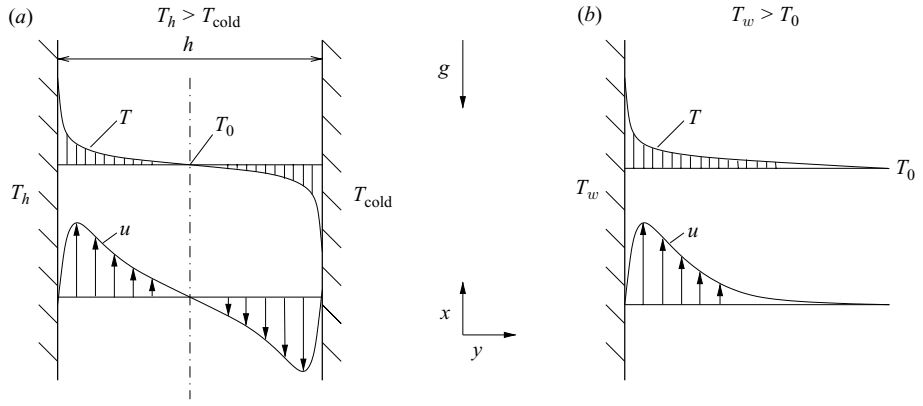


FIGURE 1. Natural convection along walls with heat transfer: (*a*) vertical channel of infinite extent (one-dimensional flow and temperature field) for example investigated by Versteegh & Nieuwstadt (1999); (*b*) hot vertical plate, measured by Tsuji & Nagano (1988*a*, *b*), Tsuji *et al.* (1991).

The first and often cited wall function approach for turbulent natural convection flows was by George & Capp (1979). They obtained a one-third power-law for temperature as well as velocity profiles after asymptotic matching of adjacent layers. The temperature profile was confirmed by Versteegh & Nieuwstadt (1999) and Henkes & Hoogendoorn (1990), for example. The velocity profile, however, was found to be inappropriate. Some shortcomings of this model will be discussed in § 4.

In a different approach, Yuan, Moser & Suter (1993) obtained wall functions by curve fitting the data of Tsuji & Nagano (1988*a*). Their functions, motivated by dimensional analysis considerations, are in good agreement with these data. There is, however, no asymptotic background for the correlations and thus no justification for applying them at higher Grashof numbers.

In our study, § 2, the temperature field is analysed asymptotically, i.e. for $Gr \to \infty$. An expression for the near-wall region as well as for the overlap layer is given. Using these results for the temperature field the velocity field can be found next, § 3, by integrating the momentum equation. In § 4 the wall functions of George & Capp (1979) will be discussed and compared to the functions we suggest as an alternative.

With an extension to mixed convection in mind our strategy is to treat natural convection flows in a way as similar as possible to that for forced convection flows.

## 2. Temperature profile

Our general approach for the natural convection temperature profile is very similar to the asymptotic analysis of forced convection flow fields. That analysis for high Reynolds numbers eventually leads to the well-known and widely accepted *logarithmic law of the wall* for turbulent velocity profiles. Though alternative approaches for forced convection end up with a power-law behaviour (cf. Barenblatt 1993*a*, *b*) highly sophisticated experiments by Zanoun, Durst & Nagib (2003) corroborate the logarithmic law. These logarithmic laws of the wall are implemented in almost all CFD codes for wall functions in order to avoid excessive grid refinement close to rigid boundaries. Avoiding terms 'right or wrong' we prefer the logarithmic law of the wall since it is well founded on asymptotic matching arguments.

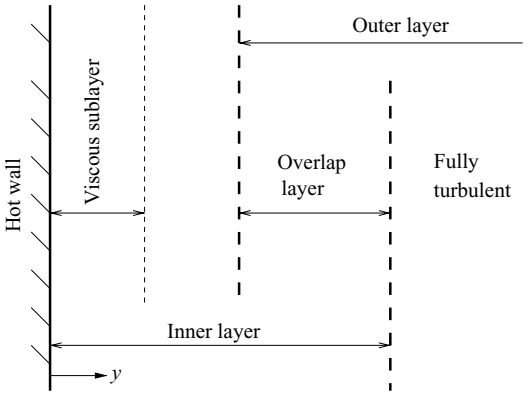


FIGURE 2. Two-layer structure of the natural convection near-wall region.

In what follows we analyse the temperature and velocity profiles of turbulent natural convection flows as closely as possible along those lines of argument that lead to the logarithmic law of the wall with forced convection flows. For reasons explained later we base our analysis on the Boussinesq approximation (constant properties with the exception of the density as a linear function of temperature, i.e. $\rho(T)$, in the buoyancy term). Table 1 below summarizes details of this approach.

The near-wall region of turbulent natural convection can generally be described by

$$0 = \frac{\partial}{\partial y}\left(\nu\frac{\partial u}{\partial y} - \overline{u'v'}\right) + g\beta(T - T_0), \tag{2.1}$$

$$0 = \frac{\partial}{\partial y}\left(a\frac{\partial T}{\partial y} - \overline{v'T'}\right), \tag{2.2}$$

see for example Tsuji & Nagano (1988*a*). Here, $y$ is the coordinate normal to the wall, $u$ the time-averaged velocity parallel to the wall, $T$ the time-averaged temperature, $T_0$ a reference temperature, $-\overline{u'v'}$ the Reynolds stress and $-\overline{v'T'}$ the turbulent heat flux. Due to the buoyancy term in the momentum equation (2.1) the two equations are linked.

First, we analyse the temperature profile assuming a two-layer structure with an inner layer and an outer layer, see figure 2. In the inner layer both modes of heat transfer, molecular and turbulent, are present. The outer layer is fully turbulent and therefore only the turbulent heat flux has to be accounted for. The heat flux in both layers is constant and equal to the wall heat flux, i.e.

$$a\frac{\partial T}{\partial y} - \overline{v'T'} = a\left.\frac{\partial T}{\partial y}\right|_w = \text{const.} \tag{2.3}$$

Here, $a\,\partial T/\partial y$ is the molecular and $-\overline{v'T'}$ the turbulent heat flux. Both together are equal to $a\,\partial T/\partial y|_w$, characterizing the heat transfer situation. Therefore a characteristic temperature $T_c$ should be based on this quantity. Furthermore, the fluid properties $a$ (or equivalently $\nu = aPr$) and $g\beta$ appear in (2.1) and (2.2) and therefore are appropriate for the definition of a characteristic temperature. Thus we obtain

$$T_c = \left(\frac{a^2}{g\beta}\left|\frac{\partial T}{\partial y}\right|_w^3\right)^{1/4} \tag{2.4}$$

The temperature difference† between the hot wall and the fluid away from it generally is $T_h - T = f(y, h, T_c, |\partial T/\partial y|_w)$. Since for $Gr \to \infty$ the thickness of the inner layer goes to zero, the finite geometrical length $h$ has no influence, so that $T_h - T = f(y, T_c, |\partial T/\partial y|_w)$. From dimensional arguments we conclude that the scale $\delta$ of the inner layer should be

$$\delta = \frac{T_c}{|\partial T/\partial y|_w}. \tag{2.5}$$

Thus, in non-dimensional variables $\Theta^\times \equiv (T_h - T)/T_c$ and $y^\times \equiv y/\delta$ the temperature takes the form

$$\Theta^\times = f(y^\times). \tag{2.6}$$

The outer layer, at least in its outer part, is affected by the geometrical length scale of the combined temperature and flow field, $h$, so that the outer non-dimensional wall distance should be $\eta \equiv y/h$. Hence in the outer layer $\Theta^\times$ takes the form

$$\Theta^\times \equiv \frac{T_h - T}{T_c} = F(\eta). \tag{2.7}$$

The temperature is non-dimensionalized with $T_c$ in both layers since $T_c$ (i.e. basically the wall heat flux) is the characteristic scale for the whole temperature field. In natural convection flows driven by wall heat transfer, temperature and velocity fields only exists as long as $T_c \neq 0$ and they vanish for $T_c \to 0$.

The inner and outer layers merge in an overlap layer in which both scalings are valid and a kind of matching, which was first introduced by Millikan (1938), can be applied. Gradients in this overlap layer scale with an intermediate variable $\hat{y} = y/(h^{1-\alpha}\delta^\alpha)$ with $0 \leqslant \alpha \leqslant 1$, i.e. $\eta \leqslant \hat{y} \leqslant y^\times$, see for example Schlichting & Gersten (2003). Temperature gradients, approaching the overlap layer from both sides, should be the same $\partial\Theta^\times/\partial\hat{y}$, i.e.

$$\frac{\partial\Theta^\times}{\partial\hat{y}} = \lim_{y^\times\to\infty} \frac{\partial\Theta^\times(y^\times)}{\partial y^\times}\frac{\partial y^\times}{\partial\hat{y}} = \lim_{y^\times\to\infty} \frac{h^{1-\alpha}\delta^\alpha}{\delta}\frac{\partial\Theta^\times(y^\times)}{\partial y^\times}, \tag{2.8}$$

$$\frac{\partial\Theta^\times}{\partial\hat{y}} = \lim_{\eta\to 0} \frac{\partial\Theta^\times(\eta)}{\partial\eta}\frac{\partial\eta}{\partial\hat{y}} = \lim_{\eta\to 0} \frac{h^{1-\alpha}\delta^\alpha}{h}\frac{\partial\Theta^\times(\eta)}{\partial\eta}. \tag{2.9}$$

Equating the two expressions leads to

$$\lim_{y^\times\to\infty} y^\times \frac{\partial\Theta^\times(y^\times)}{\partial y^\times} = \lim_{\eta\to 0} \eta\frac{\partial\Theta^\times(\eta)}{\partial\eta} \tag{2.10}$$

when both sides are multiplied by $y$.

In general, (2.10) can only be fulfilled if both sides have the same constant value $C$. Therefore

$$\lim_{y^\times\to\infty} \frac{\partial\Theta^\times(y^\times)}{\partial y^\times} = \frac{C}{y^\times} \tag{2.11}$$

which, after an integration over the inner layer, leads to

$$\lim_{y^\times\to\infty} \Theta^\times = C\ln(y^\times) + D. \tag{2.12}$$

† For a positive temperature difference one has to distinguish between hot and cold walls. Without loss of generality we use the temperature difference between the hot wall $T_h$ and the fluid $T$ so that $(T_h - T) > 0$.

| | Forced convection $Re \to \infty$ | Natural convection $Gr \to \infty$ |
|---|---|---|
| Governing equation | $\nu \dfrac{\partial u}{\partial y} - \overline{u'v'} = \nu \dfrac{\partial u}{\partial y}\bigg\vert_w$ | $a \dfrac{\partial T}{\partial y} - \overline{v'T'} = a \dfrac{\partial T}{\partial y}\bigg\vert_w$ |
| Characteristic parameter | $\nu \dfrac{\partial u}{\partial y}\bigg\vert_w = \dfrac{\tau_w}{\rho}$ | $a \dfrac{\partial T}{\partial y}\bigg\vert_w = \dfrac{q_w}{\rho c_p}$ |
| Reference quantity | $u_\tau \equiv \sqrt{\nu \dfrac{\partial u}{\partial y}\bigg\vert_w} = \sqrt{\dfrac{\tau_w}{\rho}}$ | $T_c \equiv \left( \dfrac{a^2}{g\beta} \cdot \left\vert \dfrac{\partial T}{\partial y} \right\vert_w^3 \right)^{1/4} = \left( \left[ \dfrac{q_w}{\rho c_p} \right]^3 \dfrac{1}{ag\beta} \right)^{1/4}$ |
| Parameters | $u = f(y, h, u_\tau, \partial u/\partial y\vert_w)$ | $T_h - T = f(y, h, T_c, \vert\partial T/\partial y\vert_w)$ |
| Inner layer | $u = f(y, u_\tau, \partial u/\partial y\vert_w)$ | $T_h - T = f(y, T_c, \vert\partial T/\partial y\vert_w)$ |
| | $y^+ = \dfrac{y}{\delta}; \quad \delta = \dfrac{u_\tau}{\partial u/\partial y\vert_w}$ | $y^\times = \dfrac{y}{\delta}; \quad \delta = \dfrac{T_c}{\vert\partial T/\partial y\vert_w}$ |
| | $u^+ = \dfrac{u}{u_\tau}$ | $\Theta^\times = \dfrac{T_h - T}{T_c}$ |
| Outer layer | $u = F(y, h, u_\tau)$ | $T_h - T = F(y, h, T_c)$ |
| | $\eta = \dfrac{y}{h}$ | $\eta = \dfrac{y}{h}$ |
| | $u^+ = \dfrac{u}{u_\tau}$ | $\Theta^\times = \dfrac{T_h - T}{T_c}$ |

TABLE 1. Inner- and outer-layer scaling for velocity ($Re \to \infty$) and temperature ($Gr \to \infty$)

Also Tsuji & Nagano (1988*a*) as well as Siebers *et al.* (1985) used logarithmic profiles. Their non-dimensionalization, however, was different and they gave no justification for that kind of profile.

The procedure to determine $\Theta^\times(y^\times)$ for $Gr \to \infty$ is very similar to how $u^+(y^+)$ is found for forced convection turbulent flows in the limit of $Re \to \infty$, as can be seen from table 1. For a detailed derivation of the law of the wall for forced convection see Schlichting & Gersten (2003) or Craft *et al.* (2002).

### 2.1. *Viscous sublayer*

For the region very close to the wall an explicit formulation can be found since there the turbulent heat flux is suppressed by the wall ($-\overline{v'T'} = 0$). The energy equation reduces to

$$\frac{\partial T}{\partial y} = \frac{\partial T}{\partial y}\bigg\vert_w \tag{2.13}$$

and can be integrated directly, shown again here, without loss of generality for a hot wall:

$$T_h - T = \left\vert \frac{\partial T}{\partial y} \right\vert_w y. \tag{2.14}$$

Its non-dimensional form is

$$\Theta^\times = y^\times. \tag{2.15}$$

### 2.2. *Comparison of temperature profiles*

In figure 3 DNS temperature data for the infinite channel are plotted in $\Theta^\times$, $y^\times$ variables and compared to (2.12) and (2.15). The data agree very well with the linear

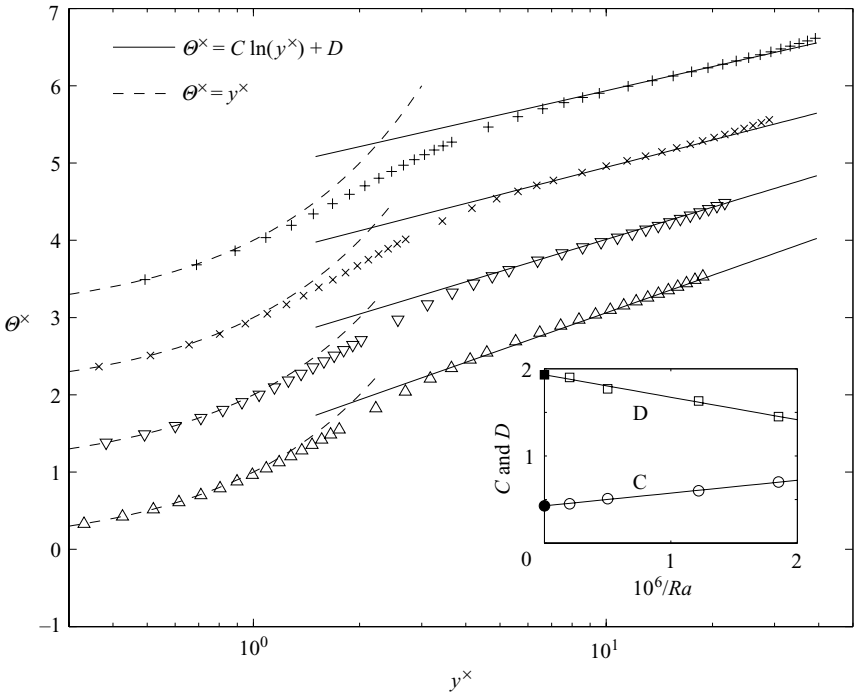


FIGURE 3. DNS temperature data from Versteegh & Nieuwstadt (1999) for the infinite channel: $Ra = 5.4 \times 10^5$ ($\triangle$), $Ra = 8.2 \times 10^5$ ($\triangledown$, shifted by 1), $Ra = 2.0 \times 10^6$ ($\times$, shifted by 2) and $Ra = 5.0 \times 10^6$ (+, shifted by 3). Also the profiles in the viscous sublayer $\Theta^\times = y^\times$ (broken line) and in the overlap layer $\Theta^\times = C\ln(y^\times) + D$ (solid line) are plotted. Due to small Rayleigh numbers each curve has its own value of $C$ and $D$. The inset shows an extrapolation for $10^6/Ra \to 0$ leading to $C_\infty = 0.427$ ($\bullet$) and $D_\infty = 1.93$ ($\blacksquare$).

temperature profiles in the viscous sublayer. In the overlap layer the data can be fitted almost perfectly to logarithmic curves when the constants $C$ and $D$ are adjusted individually for each curve, i.e. when $C$ and $D$ depend on the Rayleigh number. This, however, is not acceptable for a general asymptotic wall function. Obviously Rayleigh numbers of the DNS solutions are not yet high enough to show a perfect asymptotic behaviour ($Ra \to \infty$). Therefore we extrapolated the results in figure 3 towards $Ra \to \infty$ or, equivalently, towards $10^6/Ra \to 0$ as shown in the inset of figure 3. From that we find $C_\infty = 0.427$ and $D_\infty = 1.93$. These $C_\infty$ and $D_\infty$ should be the asymptotic constants for all natural convection flows along vertical walls in the limit $Ra \to \infty$ or $Gr \to \infty$. Thus we postulate a general overlap-layer temperature profile

$$\Theta^\times = 0.427\ln(y^\times) + 1.93. \tag{2.16}$$

Its general validity should be checked by comparing the asymptotic profile with experimental data for various other natural convection flows.

Then, however, one has to carefully take into account that (2.16) holds under the assumption of constant properties (Boussinesq approximation). Also DNS data were generated for a constant-property fluid. Measurements, however, are always subject to property variations due to non-constant temperatures. For example, in the data of Tsuji & Nagano (1988*a*), shown later in figure 4, the thermal diffusivity $a$ changes from $217.3\,\mathrm{m^2\,s^{-1}}$ (17 °C) to $271.3\,\mathrm{m^2\,s^{-1}}$ (60 °C), i.e. by about 30% in the temperature range of their measurements.

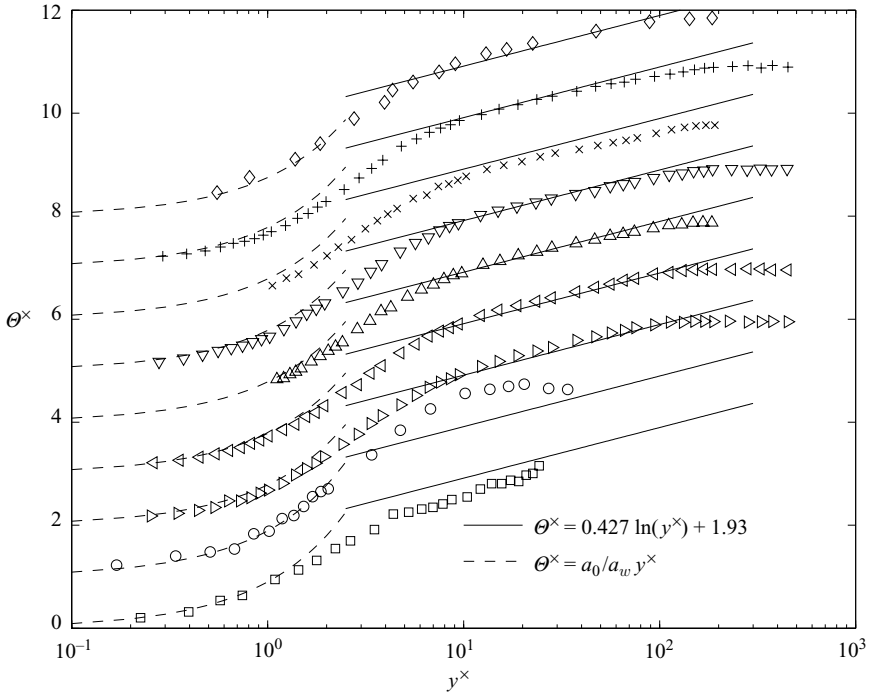


FIGURE 4. Temperature data from Betts & Bokhari (2000) for $Ra = 1.43 \times 10^6$ (□), from Ampofo & Karayiannis (2003) for $Ra = 1.59 \times 10^9$ (○), from Tsuji & Nagano (1988*a*) for $Gr_x = 1.55 \times 10^{10}$ (▷), $Gr_x = 3.62 \times 10^{10}$ (◁), $Gr_x = 7.99 \times 10^{10}$ (△), $Gr_x = 8.44 \times 10^{10}$ (▽), $Gr_x = 8.99 \times 10^{10}$ (×), $Gr_x = 17.97 \times 10^{10}$ (+) and from Cheesewright (1968) for $Gr_x = 8.65 \times 10^{10}$ (◇). To avoid confusion subsequent data sets are shifted by one temperature unit. Here $Gr_x = g\beta\Delta T x^3/\nu^2$ with $x$ being the distance from the leading edge of the vertical plate.

With DNS data of a constant-property analysis, we have to account for variable-property effects in the measured data, before we compare them to the DNS data. Since temperature gradients are very steep close to the wall, properties are almost constant away from the wall with the values of the bulk flow (index: 0). We therefore only account for the special situation with respect to the property behaviour at the wall (index: $w$). We do this by multiplying measured temperature gradients at the wall by $a_w/a_0$, which is the ratio of the thermal diffusivity at the wall and at bulk temperatures. We then have the fictitious temperature gradient that would exist if properties were constant (corresponding to the wall heat flux density of the experiment). This gradient must be used when comparing measured data to (2.16). It is incorporated in $T_c$ according to (2.4) which now reads

$$T_c = \left( \frac{a_0^2}{g\beta} \left[ \frac{a_w}{a_0} \left| \frac{\partial T}{\partial y} \right|_w \right]^3 \right)^{1/4} \tag{2.17}$$

and in $y^\times$ which now becomes

$$y^\times = \frac{y}{T_c} \left( \frac{a_w}{a_0} \left| \frac{\partial T}{\partial y} \right|_w \right). \tag{2.18}$$

In figure 4 data from various natural convection flows are shown. Since variable-property effects are present in the viscous sublayer but not in the bulk, a correction

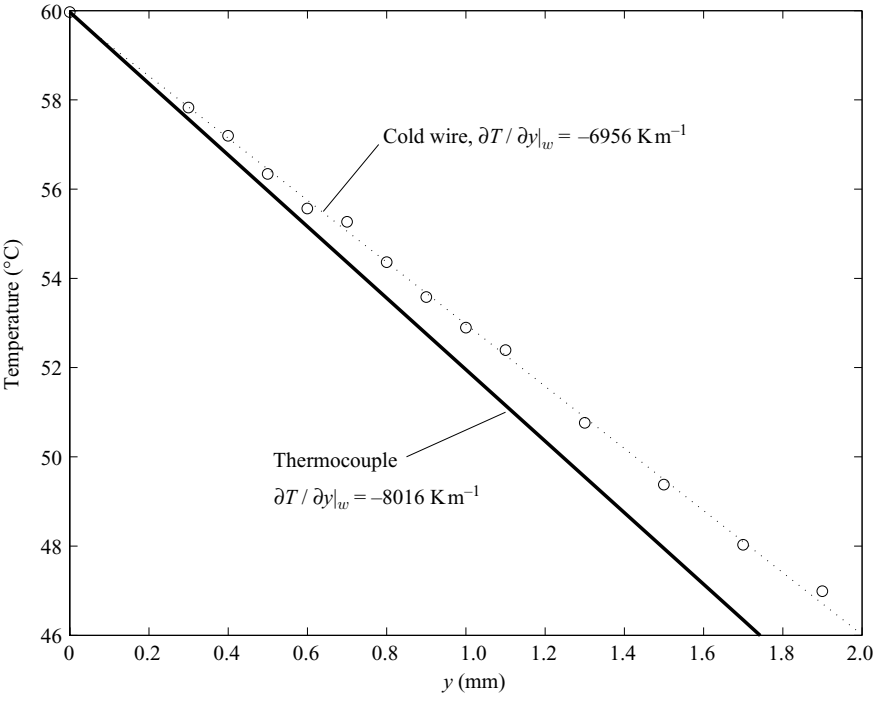


FIGURE 5. Temperature profiles near the wall for $Gr_x = 8.44 \times 10^{10}$ measured by two different methods taken from Tsuji & Nagano (1988*a*). Thermocouple (solid line) and cold wire (○) measurements with temperature gradients $\partial T/\partial y|_w$ deviating by 12 %.

factor $a_0/a_w$ explicitly appears in $\Theta^\times$ when measured data are compared to the constant-property asymptotic sublayer profile (2.15). Logarithmic behaviour is clearly shown, with the exception of the two lowest-Rayleigh-number data sets which obviously are still far away from an universal asymptotic behaviour.

Measured data in all these cases have to be analysed very carefully and error estimates are crucial. As an example figure 5 shows temperature data close to the wall from Tsuji & Nagano (1988*a*), measured by two different methods. Gradients vary by about 12% with error margins necessarily being even higher.

## 3. Velocity profile

The momentum equation for turbulent natural convection in the near-wall region, (2.1), is repeated here for convenience:

$$0 = \frac{\partial}{\partial y}\left(\nu\frac{\partial u}{\partial y} - \overline{u'v'}\right) + g\beta(T - T_0). \tag{3.1}$$

Integrating (3.1) twice leads to the velocity profiles in the viscous sublayer as well as in the overlap layer.

### 3.1. *Velocity profile in the viscous sublayer*

Very close to the wall in a purely viscous sublayer turbulent stresses $-\overline{u'v'}$ are absent due to wall damping of the velocity fluctuations. Here, the non-dimensionalized

velocity profile $U^\times = u/u_c$ can be obtained by inserting $\Theta^\times = y^\times$, $-\overline{u'v'} = 0$ and $\Theta_0^\times = (T_h - T_0)/T_c$ in the non-dimensional form of (3.1). Integration yields

$$U^\times = \frac{1}{6}y^{\times 3} - \frac{1}{2}\Theta_0^\times y^{\times 2} + \left.\frac{\partial U^\times}{\partial y^\times}\right|_w y^\times \tag{3.2}$$

with the characteristic velocity

$$u_c \equiv \frac{g\beta T_c^3}{\nu}\left|\frac{\partial T}{\partial y}\right|_w^{-2}. \tag{3.3}$$

The profiles for $U^\times$ and $\Theta^\times$ in the viscous sublayer, (3.2) and (2.15), are the same as those in George & Capp (1979) or Henkes & Hoogendoorn (1990), for example. The overlap-layer profiles, however, are different. That for the temperature has been provided by (2.16), the velocity profile will be deduced next.

### 3.2. *Velocity profile in the overlap layer*

A straightforward approach for the velocity profiles, adopted by George & Capp (1979), for example, would be to match velocity gradients in the overlap layer, see figure 2. As shown by Versteegh & Nieuwstadt (1999) this, however, leads to an insufficient representation of the flow field.

Alternatively, the momentum equation can be the starting point for determining the asymptotic form of the flow field. Since matching occurs in the overlap layer, the momentum equation can be taken as that of the inner layer, i.e. (3.1), neglecting the viscosity influence, which 'dies out' further away from the wall. Hence we have

$$0 = -\frac{\partial \overline{u'v'}}{\partial y} + g\beta(T - T_0). \tag{3.4}$$

Since we want to find an asymptotic representation for the time-mean velocity $u$, turbulence closure is required. This can be applied on various levels and will provide an asymptotic representation of $u$ based on turbulence closure according to that level.

Since most CFD codes (in which wall functions should be implemented) use an eddy-viscosity turbulence closure we adopt this and in non-dimensional form obtain

$$0 = \frac{\partial}{\partial y^\times}\left(\frac{\nu_t}{\nu}\frac{\partial U^\times}{\partial y^\times}\right) - \Theta^\times + \Theta_0^\times \tag{3.5}$$

from (3.4).

Solution of this equation is straightforward once $\Theta^\times(y^\times)$ and $\nu_t(y^\times)$ are known. In § 2 an expression for $\Theta^\times(y^\times)$ in the overlap layer was derived and can be applied, see (2.12). The eddy viscosity $\nu_t(y^\times)$ can be linked to the turbulent thermal diffusivity $a_t(y^\times)$ by the turbulent Prandtl number $\sigma_t = \nu_t/a_t$ through

$$\frac{\nu_t}{\nu} = \frac{a_t}{a}\frac{\sigma_t}{Pr}. \tag{3.6}$$

When $\sigma_t$ is known the set of equations is closed and can be solved. We now assume the temperature fluctuations to be those of a passive scalar what reasonably accounts for the physics of buoyancy-induced turbulence. Since then $a_t$ is intimately linked to $\nu_t$ (both coefficients are the mean flow and mean temperature representation of turbulence effects) their ratio will be (almost) constant.

As an example, the inset in figure 7 below shows a plot of the turbulent Prandtl number $\sigma_t$ obtained from the DNS data of Versteegh & Nieuwstadt (1999). Experimental data (e.g. Tsuji & Nagano 1988*a*) show too high fluctuations in the

measured gradients to be used here. For $y^\times \gtrsim 9$ the turbulent Prandtl number is almost constant with $\sigma_t \approx 0.9$ like in many forced convection flows. The singular behavior of $\sigma_t$ near the wall (where $\partial u/\partial y = 0$ but $\partial T/\partial y \neq 0$) does not pose a problem since it is not in the $y^\times$-range of interest. Thus, the constant-turbulent-Prandtl-number concept, here with $\sigma_t = 0.9$, is used for natural convection in the overlap layer.

With $a_t = -\overline{v'T'}/(\partial T/\partial y)$, assuming that $a_t \gg a$ in the overlap layer the energy equation (2.3) in non-dimensional form is

$$\frac{a_t}{a}\frac{\partial \Theta^\times}{\partial y^\times} = 1. \tag{3.7}$$

With $\partial \Theta^\times/\partial y^\times = C/y^\times$ according to (2.11) we thus immediately find $a_t/a = y^\times/C$ and therefore

$$\frac{\nu_t}{\nu} = \frac{\sigma_t y^\times}{CPr}. \tag{3.8}$$

Inserting (3.8) and (2.12) into the momentum equation (3.5), it becomes

$$\frac{\partial}{\partial y^\times}\left(\frac{\sigma_t y^\times}{CPr}\frac{\partial U^\times}{\partial y^\times}\right) = C\ln(y^\times) + D - \Theta_0^\times. \tag{3.9}$$

It can be integrated twice with respect to $y^\times$ and leads to the velocity profile in the overlap layer:

$$U^\times = \frac{CPr}{\sigma_t} y^\times \left(C[\ln(y^\times) - 2] + D - \Theta_0^\times\right) + E\ln(y^\times) + F \tag{3.10}$$

Though $E$ and $F$ are constants with respect to $y^\times$ they may depend on parameters like $\Theta_0^\times$ and the wall gradient $\partial U^\times/\partial y^\times|_w$, which both are parameters in the non-dimensional form of the velocity distribution (3.2) in the viscous sublayer. Since $\Theta_0^\times$ appears in $U^\times$ already, see (3.10), we tentatively assume $E$ and $F$ to be parametrically dependent on $\partial U^\times/\partial y^\times|_w$ only, with the simple form $E = e_1 \partial U^\times/\partial y^\times|_w + e_2$ and $F = f_1 \partial U^\times/\partial y^\times|_w + f_2$.

### 3.3. *Comparison of velocity profiles*

In order to end up with general asymptotic wall functions, $E$ and $F$ in (3.10) have to be determined. We do that by adjusting them to experimental velocity data (flat plate, cavity, figure 6) and then demonstrate that they also hold for DNS solutions (infinite channel, figure 7).

Again the problem arises that experiments are always subject to variable-property effects whilst DNS data assume constant-property physics (Boussinesq approximation).

As for the temperature profile we therefore assume a bulk value for the kinematic viscosity, $\nu_0$, further away from the wall (i.e. in the overlap layer) and a factor $\nu_0/\nu_w$ appears in the representation of the velocity profile in the sublayer when it is compared to experimental data. Instead of (3.2) we then have

$$U^\times = \frac{\nu_0}{\nu_w}\left(\frac{1}{6}\frac{a_0}{a_w} y^{\times 3} - \frac{1}{2}\Theta_0^\times y^{\times 2}\right) + \left.\frac{\partial U^\times}{\partial y^\times}\right|_w y^\times \tag{3.11}$$

with the characteristic velocity $u_c$ as

$$u_c = \frac{g\beta T_c^3}{\nu_0}\left(\frac{a_w}{a_0}\left|\frac{\partial T}{\partial y}\right|_w\right)^{-2} \tag{3.12}$$

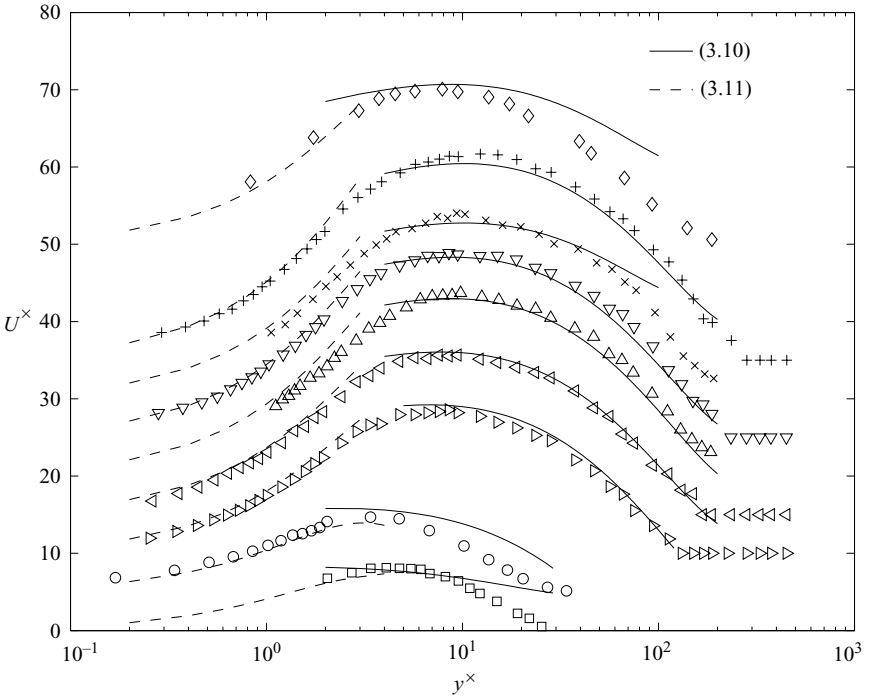


FIGURE 6. Velocity data from Betts & Bokhari (2000) for $Ra = 1.43\times10^6$ (□), from Ampofo & Karayiannis (2003) for $Ra = 1.59\times10^9$ (○), from Tsuji & Nagano (1988*a*) for $Gr_x = 1.55\times10^{10}$ (▷), $Gr_x = 3.62\times10^{10}$ (◁), $Gr_x = 7.99\times10^{10}$ (△), $Gr_x = 8.44\times10^{10}$ (▽), $Gr_x = 8.99\times10^{10}$ (×), $Gr_x = 17.97\times10^{10}$ (+) and from Cheesewright (1968) for $Gr_x = 8.65\times10^{10}$ (◇). To avoid confusion subsequent data sets are shifted by five velocity units.

and $T_c$ according to (2.17).

Figure 6 shows measured flat-plate and cavity data from which

$$E = 0.49\frac{\nu_w}{\nu_0}\left.\frac{\partial U^\times}{\partial y^\times}\right|_w - 2.27\,, \tag{3.13}$$

$$F = 1.28\frac{\nu_w}{\nu_0}\left.\frac{\partial U^\times}{\partial y^\times}\right|_w + 1.28 \tag{3.14}$$

are determined by adjusting the overlap layer profile (3.10) taking variable-property effects into account. Only for the lowest Rayleigh numbers is (3.10) a poor representation of the experimental data, as previously obtained for the temperature profile. Viscous sublayer profiles compared to (3.11) show good agreement.

Applying $E$ and $F$ according to (3.13) and (3.14), the infinite channel DNS data, see figure 7, are represented quite well for the high-Rayleigh-number cases. The viscous sublayer is now compared to (3.2) since DNS data are for constant properties.

Table 2 summarizes the near-wall analytical functions (2.12), (2.15), (3.2) and (3.10) and the constants therein.

Cheesewright (1986) as cited in Henkes & Hoogendoorn (1990) also proposed a logarithmic temperature wall function and a velocity profile similar to (3.10). This, however, is based on a different non-dimensionalization of the basic equations.

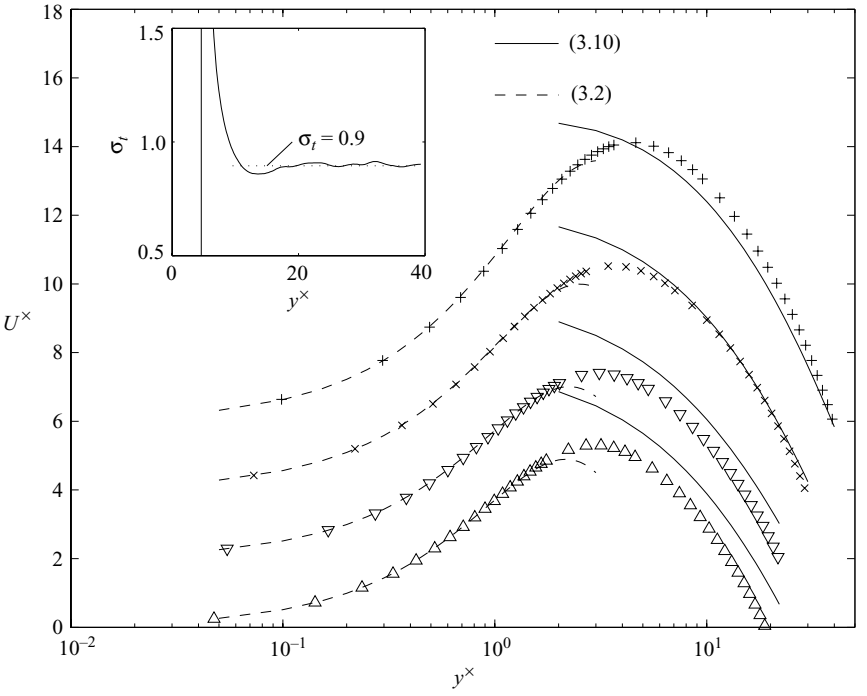


FIGURE 7. DNS velocity data from Versteegh & Nieuwstadt (1999) for the infinite channel: $Ra = 5.4 \times 10^5$ ($\triangle$), $Ra = 8.2 \times 10^5$ ($\triangledown$, shifted by 2), $Ra = 2.0 \times 10^6$ ($\times$, shifted by 4) and $Ra = 5.0 \times 10^6$ ($+$, shifted by 6). The inset shows $\sigma_t = \nu_t/a_t$ as a function of $y^\times$ for $Ra = 5.0 \times 10^6$ where $\sigma_t \approx 0.9$ for $y^\times > 9$.

| Layer | Temperature $\Theta^\times$ | Velocity $U^\times$ |
|---|---|---|
| Viscous sublayer | $y^\times$ | $\frac{1}{6}y^{\times 3} - \frac{1}{2}\Theta_0^\times y^{\times 2} + \left.\frac{\partial U^\times}{\partial y^\times}\right\|_w y^\times$ |
| Overlap layer | $C\ln(y^\times) + D$ | $\frac{C\mathrm{Pr}}{\sigma_t} y^\times \left( C[\ln(y^\times) - 2] + D - \Theta_0^\times \right) + E\ln(y^\times) + F$ |

with:

| $C$ | $D$ | $E$ | $F$ |
|---|---|---|---|
| 0.427 | 1.93 | $0.49 \left.\frac{\partial U^\times}{\partial y^\times}\right\|_w - 2.27$ | $1.28 \left.\frac{\partial U^\times}{\partial y^\times}\right\|_w + 1.28$ |

TABLE 2. Analytical functions for temperature and velocity in the viscous sublayer and the overlap layer of turbulent natural convection flows (constant properties). The functions shown above in the overlap layer can be used as wall functions in CFD codes.

## 4. Wall functions by George & Capp

The study of George & Capp (1979) is frequently referred to as a 'standard' when wall functions for turbulent natural convection are used, see for example Schlichting & Gersten (2003).

Like in our study George & Capp (1979) subdivided the natural convection boundary layers into an inner layer (molecular and turbulent transport) and an outer layer with only turbulent transport of momentum and thermal energy. In

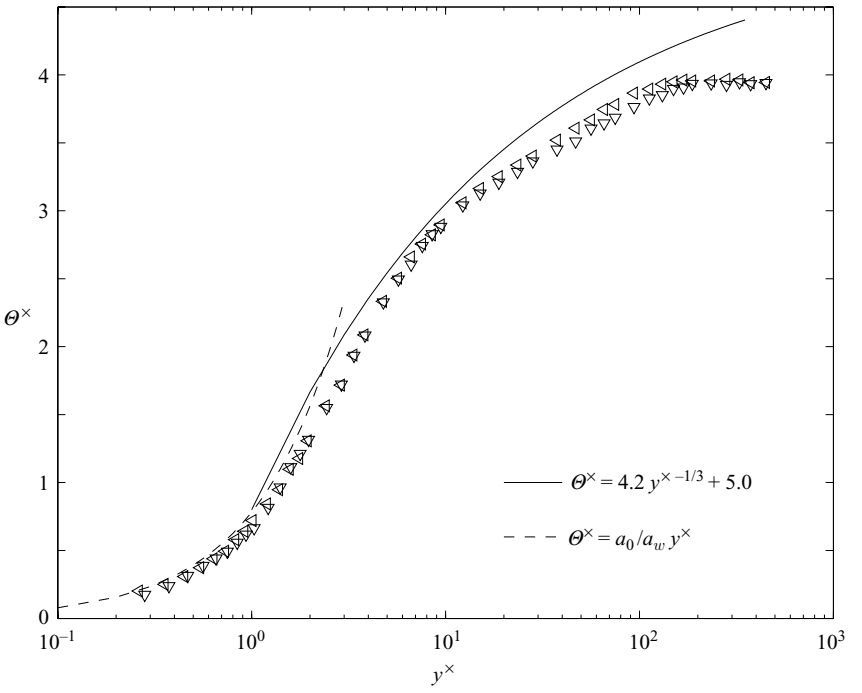


FIGURE 8. Temperature wall function (4.1, solid line) of George & Capp (1979) with constants proposed by Versteegh & Nieuwstadt (1999) compared to data of Tsuji & Nagano (1988*a*) for $Gr_x = 3.62 \times 10^{10}$ ($\triangleleft$) and $Gr_x = 8.44 \times 10^{10}$ ($\triangledown$).

contrast to our study, however, they chose different characteristic temperatures ($T_{c,i}$ and $T_{c,o}$) and velocities ($u_{c,i}$ and $u_{c,o}$) for the inner and outer layers, respectively.

Since their viscous sublayer profiles for the temperature and velocity are basically the same as those we found (see (2.15) and (3.2)) we only compare profiles in the overlap layer.

Due to the different non-dimensionalization of George & Capp (1979), matching of the inner and outer layers leads to a different temperature profile compared to our profile (2.12). Their temperature profile for the overlap layer is

$$\Theta^\times = K_2 y^{\times -1/3} + A(Pr). \tag{4.1}$$

At that time George & Capp (1979) were not able to give reliable values for their constants. Therefore, $K_2 = -4.2$ and $A = 5.0$ are used, which Versteegh & Nieuwstadt (1999) determined by adjusting the profiles of George & Capp (1979) to their DNS data. The wall function (4.1) deviates appreciably from the data of Tsuji & Nagano (1988*a*), for example, see figure 8.

For the velocity in the overlap layer, they obtain a function†

$$\frac{U^\times}{Pr} = K_1 \cdot y^{\times 1/3} + B(Pr) \tag{4.2}$$

instead of our (3.10). Since $K_1$ is a constant in their study ($K_1 = 27$) all flows with the same Prandtl number ($B(Pr)$ fixed) are then represented by a single function $U^\times(y^\times)$.

† George & Capp (1979) used a slightly different non-dimensionalization so that instead of $U^\times = u/u_c$ the left-hand side is $U^\times/Pr$.

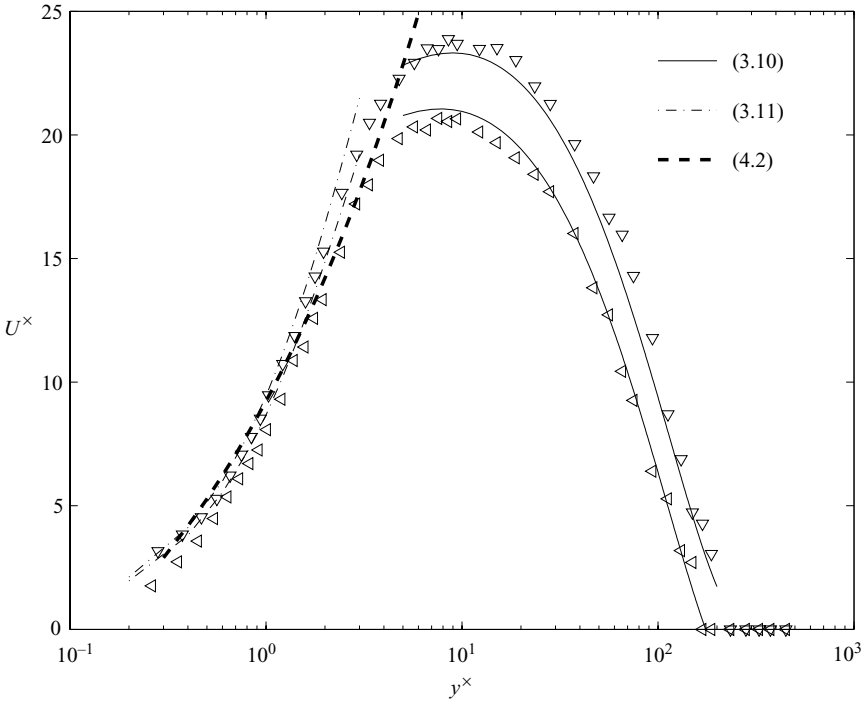


FIGURE 9. Velocity wall function (4.2) of George & Capp (1979) compared to data of Tsuji & Nagano (1988*a*) for $Gr_x = 3.62 \times 10^{10}$ ($\triangleleft$) and $Gr_x = 8.44 \times 10^{10}$ ($\triangledown$), also shown: our velocity profiles (3.11) in the viscous sublayer and (3.10) in the overlap layer.

Figure 9 shows two measured velocity profiles from Tsuji & Nagano (1988*a*), both for $Pr = 0.71$: the profile (3.11) in the viscous sublayer and the velocity function (4.2) by George & Capp (1979). Though (4.2) should cover the overlap layer it is only a reasonable representation of the velocity profile for $y^\times < 3$. This near-wall region is very well represented by the viscous sublayer velocity profile (3.11) already.

Very different from the profile (4.2), our overlap-layer profile (wall function) (3.10) covers the $y^\times$-region $3 < y^\times < 200$.

## 5. Conclusions

Based on asymptotic considerations for the near-wall region in turbulent natural convection flows new analytical functions have been derived for the asymptotic temperature and velocity profiles.

In determining constants by comparing the asymptotic profiles to measured data it is crucial to take into account variable-property effects.

If this is done one obtains a general form for velocity and temperature profiles that hold for all kinds of turbulent natural convection flows close to vertical walls. Unlike previous attempts they can cover almost the whole boundary layer. They can be incorporated in CFD codes to avoid the otherwise necessary fine grids close to the wall when Grashof (or Rayleigh) numbers are high. Since then the numerical solution does not reach the wall (the remaining distance is bridged by the wall functions) it is advantageous to have wall function profiles that are based on bulk property values (with the wall-property-value influence incorporated indirectly by the way its

constants are determined from experimental data). Variable-property effects can also explain deviations between DNS and experimental data often found in the literature.

## REFERENCES


Ampofo, F. & Karayiannis, T. G. 2003 Experimental benchmark data for turbulent natural convection in an air filled square cavity. *Intl J. Heat Mass Transfer* **46**, 3551–3572.

Barenblatt, G. I. 1993*a* Scaling laws for fully developed shear flow. Part 1. Basic hypotheses and analysis. *J. Fluid Mech.* **248**, 513–520.

Barenblatt, G. I. 1993*b* Scaling laws for fully developed shear flow. Part 2. Processing of experimental data. *J. Fluid Mech.* **248**, 521–529.

Betts, P. L. & Bokhari, I. H. 2000 Experiments on turbulent natural convection in an enclosed tall cavity. *Intl J. Heat Fluid Flow* **21**, 675–683.

Boudjemadi, R., Mapu, V., Laurence, D. & Le Quere, P. 1997 Budgets of turbulent stresses and fluxes in a vertical slot natural convection flow at Rayleigh $Ra = 10^5$ and $5.4 \times 10^5$. *Intl J. Heat Fluid Flow* **18**, 70–79.

Cheesewright, R. 1968 Turbulent natural convection from a vertical plane surface. *J. Heat Transfer* **90**, 1–8.

Cheesewright, R. 1986 The scaling of turbulent natural convection boundary layers in the asymptotic limit of infinite Grashof number. *Paper presented atEuromech Colloquium 207, 7–9 April, Delft, The Netherlands.*

Cheesewright, R., King, K. J. & Ziai, S. 1986 Experimental data for the validation of computer codes for the prediction of two-dimensional buoyant cavity flows. *Proc. ASME Meeting HTD* **60**, 75–86.

Craft, T. J., Gerasimov, A. V., Iacovides, H. & Launder, B. E. 2002 Progress in the generalization of wall-function treatments. *Intl J. Heat Fluid Flow* **23**, 148–160.

George, W. K. & Capp, S. P. 1979 A theory for natural convection turbulent boundary layers next to heated vertical surfaces. *Intl J. Heat Mass Transfer* **22**, 813–826.

Henkes, R. A. W. M. & Hoogendoorn, C. J. 1990 Numerical determination of wall functions for the turbulent natural convection boundary layer. *Intl J. Heat Mass Transfer* **33**, 1087–1097.

Millikan, C. B. 1938 A critical discussion of turbulent flows in channels and circular tubes. *Proc. 5th Int. Congress of Applied Mechanics*, pp. 386–392. MIT Press.

Schlichting, H. & Gersten, K. 2003 *boundary-layer Theory*. Springer.

Siebers, D. L., Moffatt, R. F. & Schwind, R. G. 1985 Experimental, variable properties natural convection from a large, vertical, flat surface. *J. Heat Transfer* **107**, 124–132.

Tsuji, T. & Nagano, Y. 1988*a* Characteristics of a turbulent natural convection boundary layer along a vertical flat plate. *Intl J. Heat Mass Transfer* **31**, 1723–1734 (data taken from www.ercoftac.org).

Tsuji, T. & Nagano, Y. 1988*b* Turbulence measurements in a natural convection boundary layer along a vertical flat plate. *Intl J. Heat Mass Transfer* **31**, 2101–2111 (data taken from www.ercoftac.org).

Tsuji, T., Nagano, Y. & Tagawa, M. 1991 Thermally driven turbulent boundary layer. *8th Symposium on Turbulent Shear Flows, Technical University of Munich*, Vol. 2, pp. 24.3.1–24.3.6 (data taken from www.ercoftac.org).

Versteegh, T. A. M. & Nieuwstadt, F. T. M. 1999 A direct numerical simulation of natural convection between two infinite vertical diffentially heated walls: scaling laws and wall functions. *Intl J. Heat Mass Transfer* **42**, 3673–3693. (DNS data taken from www.ercoftac.org).

Wang, M., Fu, S. & Zhang, G. 2002 Large-scale spiral structures in turbulent thermal convection between two vertical plates. *Phys. Rev.* E **66**, 066306.

Yuan, X., Moser, A. & Suter, P. 1993 Wall functions for numerical simulation of turbulent natural convection along vertical plates. *Intl J. Heat Mass Transfer* **36**, 4477–4486.

Zanoun, E.-S., Durst, F. & Nagib, H. 2003 Evaluating the law of the wall in two-dimensional fully developed turbulent channel flows. *Phys. Fluids* **15**, 3079–3089.